Spherically-Actuated Platform Manipulator

Robert L. Williams II
Dana B. Poling
Department of Mechanical Engineering
Ohio University
Athens, Ohio

DETC2000/MECH-6504
2000 ASME Design Technical Conferences
26th Biennial Mechanisms Conference
Parallel Manipulator Design, Path Planning, and Control
September 10-13, 2000, Baltimore, MD

CONTACT AUTHOR INFORMATION:
Robert L. Williams II
Department of Mechanical Engineering
257 Stocker Center
Ohio University
Athens, OH 45701-2979
phone: (740) 593-1096
fax: (740) 593-0476
email: bobw@bobcat.ent.ohiou.edu
URL: http://www.ent.ohiou.edu/~bobw

Proceedings of DETC2000
2000 ASME Design Engineering Technical Conference
September 10-13, 2000, Baltimore, MD

DETC2000/MECH-6504

SPHERICALLY-ACTUATED PLATFORM MANIPULATOR

Robert L. Williams II and Dana B. Poling
Ohio University
Athens, OH 45701

ABSTRACT

This paper presents the inverse and forward pose kinematics solutions for a novel 6-dof platform manipulator, actuated by two base-mounted spherical actuators. The moving platform is connected to the fixed base by two identical *SPU* (alternatively, *SRU*) serial chain legs. The *S*-joint is active, and remaining two joints in each chain are passive. The numerical Newton-Raphson technique is employed to solve the pose problems. Unfortunately, the passive joint variables cannot be ignored in the pose kinematics solutions as they can for the Gough/Stewart platform. Examples are presented and hardware has been built, using two Rosheim Omni-Wrists on loan from NASA.

1. INTRODUCTION

Parallel robots have been proposed for some time now, due to their potential advantages over serial robots in high load bearing, acceleration, and stiffness, with lower moving mass. A prime disadvantage is reduced workspace relative to serial robots. Hunt (1983) did some of the pioneering work in this field. Tsai (1999) has recently published a book giving a good overview of the mechanics of parallel robots.

A major type of parallel robot architecture is platform manipulators such as the well-known Gough/Stewart platform (Stewart, 1966). This 6-degree-of-freedom (dof) platform is controlled by six prismatic legs, connecting the moving platform in parallel with the base. Interestingly, this platform architecture that has become known as the Stewart platform never appears in Stewart (1966). A related architecture is the variable-geometry truss (VGT), such as the double-octahedral design from NASA (Rhodes and Mikulas, 1985). These two types of parallel robot are designed to be loaded axially only; prismatic actuators are generally the control elements, and passive *U* and *S* joints are included to allow the proper freedoms. These types of manipulators have been proposed and used in such applications as flight simulation, machining tools, assembly fixturing, entertainment, space structure modules, and robotic joints for long-reach manipulators.

Many spherical actuation devices have been built or proposed; most of these are developed for use as robotic wrist mechanisms (e.g. the offset "spherical" Omni-Wrist (Rosheim, 1987) and the truly spherical robot wrists of Roth and Lee (1995), and Stanisic and Duta (1990)). More recently, various spherical motors have been developed (e.g. Wang et al., 1998, Lee et al., 1996).

The idea that led to the platform manipulator presented in this paper is that the (generally passive) spherical joints of a platform manipulator may be instead actively driven; then the remaining *P*, *U*, and other joints are passive. Two active *S* joints are sufficient for a 6-dof platform manipulator. In this paper we introduce the SPherically-Actuated platform Manipulator, or SPAM for short. According to a search of the literature, this idea has not been presented before.

This paper focuses on the inverse and forward pose (position and orientation) kinematics solution for SPAM. First, the new platform manipulator architecture is presented, followed by solution of the inverse and forward pose kinematics problems. Trajectory examples are then presented to demonstrate these solutions.

2. PLATFORM MANIPULATOR DESCRIPTION

The parallel platform manipulator presented in this paper (SPherically-Actuated platform Manipulator, SPAM) consists of a fixed base and a moving platform connected by two serial chain legs. The platform is actuated by two spherical actuators mounted to the base. Two variations are considered: 1) Two *SPU* (spherical-prismatic-universal joint) serial chain legs, as shown in the CAD model of Fig. 1; and 2) Two *SRU* (spherical-revolute-universal joint) serial chain legs, as shown in the CAD model of Fig. 2. In both cases, the *S* joints are actively actuated while the remaining leg joints are passive. The *U* joints are fixed to the moving platform, while the *P* (or *R*) joints are between the *S* and *U* joints.

The two manipulator versions are very similar; the only difference is in the kinematics of the passive *R* joint vs. the passive *P* joint. For both versions, the mobility is calculated with the Kutzbach equation:

$$M = 6(N-1) - 5J_1 - 4J_2 - 3J_3$$
$$M = 6(6-1) - 5(2) - 4(2) - 3(2) = 6 \qquad (1)$$

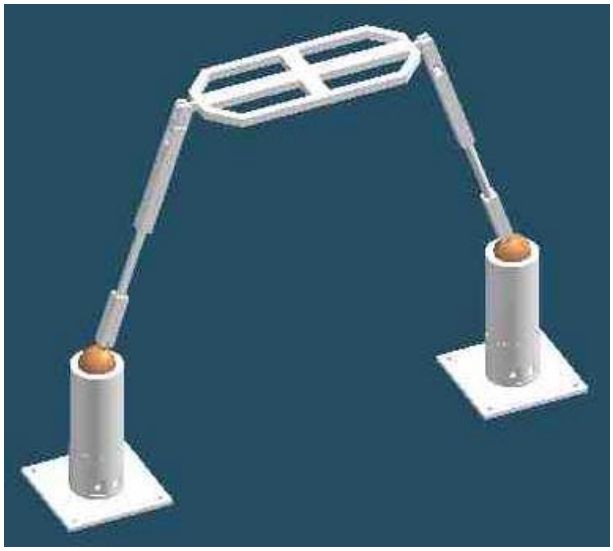

Figure 1. Platform Manipulator, SPU *Version*

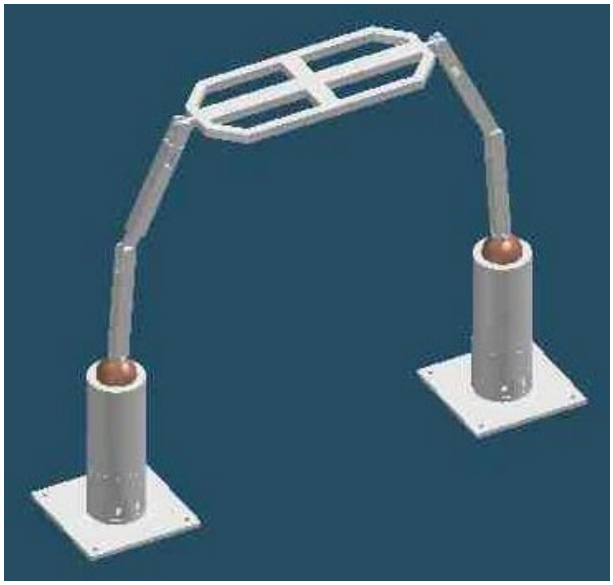

Figure 2. Platform Manipulator, SRU *Version*

Thus, this platform manipulator has 6 degrees-of-freedom (dof), actively provided by the two base-mounted 3-dof spherical actuators. By controlling the six spherical joint variables, general Cartesian poses (positions and orientations) may be reached within a limited workspace. Additional constraining serial legs may be used, with all passive joints or another *S* actuator (redundant actuation).

In our platform manipulator design, the two spherical actuators are two Rosheim Omni-Wrists (Rosheim, 1987), on loan from NASA Langley Research Center (see Fig. 3). These robot wrists, originally developed for Space Station robots, are singularity-free, stiff, and capable of bearing high loads. Each wrist provides $\pm 90^\circ$ in *pitch* and *yaw* motions, plus continuous, bi-directional *roll* motion. These wrists are not truly spherical since there is a wrist offset separating two sets of revolute axes; the kinematics of our platform manipulator are significantly simplified if truly spherical actuators are used (such as those presented by Stanisic and Duta, 1990; and Lee et al., 1996).

Figure 3. 3-dof Omni Wrist

The forward and inverse pose and rate kinematics solutions with singularity analysis have been presented for the Omni-Wrist standing alone (Williams, 1990) and for the Omni-Wrist mounted as the wrist mechanism in a serial robot chain (Williams, 1999). The idea that led to the project described in this paper is that the Omni-Wrist (or other spherical actuator) can be used as an active spherical joint in a parallel platform-type manipulator; *S* joints are traditionally passive, rather than active, in parallel robots.

Just like the potted meat substitute, our SPAM robot may not be the most desirable platform robot architecture. In more established platform manipulators such as the Gough/Stewart Platform (Stewart, 1966) and variable geometry trusses (Rhodes and Mikulas, 1985), the robot is designed such that all loads are axial, avoiding by design the moment loading. This is not the case with our active spherically-driven platform; however, other platform manipulators from the literature with *R*-joint actuation suffer from this deficit as well. Also, as stated previously, the Omni-Wrist is built to handle large moment loading. Another SPAM shortcoming is that the inverse pose kinematics is not straight-forward as it is for the Gough/Stewart platform. Despite these issues, we present the SPAM concept to explore spherical actuation of platform manipulators, due to the recent interest in development of spherical actuators. The main focus of this paper is SPAM pose (position and orientation) kinematics, presented in the next section.

3. POSE KINEMATICS

This section presents the inverse and forward pose (position and orientation) kinematics analysis for the SPAM robot. Inverse pose kinematics is required for platform control, and forward pose kinematics is required for platform simulation and sensor-based control. Pose kinematics is concerned with relating the active joint variables and the Cartesian pose variables for the platform. Unfortunately, there are also passive, intermediate joint variables which are unknowns in both forward and inverse pose, and which complicate these problems.

In this section we focus on the *SPU* version of SPAM. The *SRU* version is very similar; details for this are presented in the Appendix. The SPAM kinematic diagram, *SPU* version, is given in Fig. 4.

Figure 4 clearly shows the offset L_2 in the "spherical" Omni-Wrist actuators. L_1 is the distance from the base frame {*B*} origin to the fixed location of the left Omni-Wrist. L_3 is the total variable length between the *S* and *U* joints; this is the length variable of the passive *P* joint. L_5 is the fixed distance between the moving platform frame {*P*} origin and the *U*-joint location of the left *SPU* leg. The platform manipulator is designed with symmetry for the left and right legs, so lengths L_1, L_2, and L_5 also appear on the right *SPU* leg. However, the right *SPU* leg passive *P* joint length is in general different from L_3, given the name L_4.

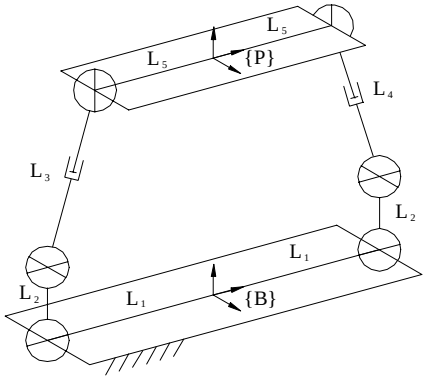

Figure 4. SPAM Kinematic Diagram, SPU *Version*

The detailed kinematic diagram for the left *SPU* serial chain leg is shown in Fig. 5. Figure 5 shows the *X* and *Z* axes for all intermediate coordinate frames, defined according to standard Denavit-Hartenberg parameters for serial robots (Craig, 1989). The Omni-Wrist active joint variables are roll θ_1, yaw θ_2, and pitch θ_3. As shown, the Omni-Wrist transfers θ_2 and θ_3 to equal rotations about the upper gimbal, offset by fixed length L_2; this is accomplished by gearing. The passive joint variables are *P*-joint length L_3 and *U*-joint angles ϕ_2 and ϕ_3. Note the *U*-joint cannot be aligned so that one of its revolute joints is along L_5, in the Y_P direction, or the platform would revolve uncontrollably about this axis (assuming the right *SPU* leg is identical). The Denavit-Hartenberg (DH) parameters (Craig, 1989) for the left *SPU* serial chain leg are given in Table I (angle units are *deg*).

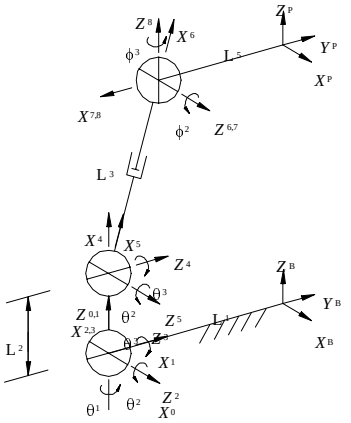

Figure 5. Left SPU *Leg Kinematic Diagram*

Table I. Left *SPU* Leg DH Parameters

i	α_{i-1}	a_{i-1}	d_i	θ_i
1	0	0	0	θ_1+90
2	90	0	0	θ_2+90
3	90	0	0	θ_3
4	0	L_2	0	θ_3
5	-90	0	0	θ_2
6	0	L_3	0	0
7	0	0	0	ϕ_2+90
8	90	0	0	ϕ_3

Due to the nature of the Omni-Wrist coupling between the two yaw and two pitch axes, θ_2 and θ_3 each appear twice in Table I, but are the same variable. Thus, though there are 8 lines of DH parameters, the *SPU* leg as a serial chain has only 6-dof, as expected. Fixed lengths L_1 and L_5 do not appear in Table I, which only relates the Omni-Wrist base to the *U* joint location; these two lengths are included via homogeneous transformation matrices later.

In our design the right *SPU* leg is identical to the left (note: not mirror image, but identical), using the following variable substitutions:

$$\theta_4 \to \theta_1 \qquad L_4 \to L_3$$
$$\theta_5 \to \theta_2 \qquad \phi_5 \to \phi_2$$
$$\theta_6 \to \theta_3 \qquad \phi_6 \to \phi_3$$

The table of DH parameters for the right *SPU* leg is thus identical to Table I, using the above substitutions.

In this section we use a combination of serial chain and parallel chain methods to formulate and solve the SPAM pose kinematics problems. The six SPAM active joint variables are left and right Omni-Wrist variables $\{\theta_1,\theta_2,\theta_3\}$ and $\{\theta_4,\theta_5,\theta_6\}$, respectively. The six Cartesian pose variables are $\{x,y,z,\alpha,\beta,\gamma\}$, related to the homogeneous transformation matrix of the moving platform frame {*P*} with respect to the fixed base frame {*B*} as given in (2):

$$ {}^B_P T = \begin{bmatrix} & \left[{}^B_P R\right] & & \left\{{}^B P_P\right\} \\ 0 & 0 & 0 & 1 \end{bmatrix}$$

$$ {}^B_P T = \begin{bmatrix} c\alpha c\beta & -s\alpha c\gamma + c\alpha s\beta s\gamma & s\alpha s\gamma + c\alpha s\beta c\gamma & x \\ s\alpha c\beta & c\alpha c\gamma + s\alpha s\beta s\gamma & -c\alpha s\gamma + s\alpha s\beta c\gamma & y \\ -s\beta & c\beta s\gamma & c\beta c\gamma & z \\ 0 & 0 & 0 & 1 \end{bmatrix} \qquad (2)$$

Where α,β,γ are *Z-Y-X* Euler angles (Craig, 1989). The six intermediate variables are left and right *SPU* leg passive variables $\{L_3,\phi_2,\phi_3\}$ and $\{L_4,\phi_5,\phi_6\}$, respectively.

Now we formulate and solve the SPAM inverse and forward pose kinematics problems using the kinematic diagrams, Denavit-Hartenberg parameters, and variables described.

3.1 Inverse Pose Kinematics

The SPAM inverse pose kinematics problem is stated: Given the desired Cartesian platform pose $\{x,y,z,\alpha,\beta,\gamma\}$ (or, equivalently,

${}^B_P T$), calculate the required Omni-Wrist actuator joint variables $\{\theta_1, \theta_2, \theta_3\}$ and $\{\theta_4, \theta_5, \theta_6\}$. The left- and right-leg passive joint variables $\{L_3, \phi_{2,} \phi_3\}$ and $\{L_4, \phi_{5,} \phi_6\}$ are also unknowns. The passive variables are not required for real-time control, but they may be used in on-line rate and dynamics equations, plus off-line for simulation.

This inverse pose problem is solved by considering the left and right *SPU* serial chain legs separately. The given Cartesian pose ${}^B_P T$ must be reached by both legs independently, each with three active and three passive joints. Thus, the problem decouples between the left and right legs.

Inverse pose kinematics is a well-known problem in serial robotics, and analytical solutions are generally preferred where possible. However, for the *SPU* serial chain using the offset Omni-Wrist actuator, analytical solutions may not exist. One could follow the combined analytical/iterative approach in Williams (1999) to solve the inverse pose kinematics of each *SPU* leg with offset Omni-Wrist. We choose instead to solve the inverse problems numerically using Newton-Raphson iteration. Below we describe the procedure for the left *SPU* leg; the right is the same, with the above-noted variable substitutions.

To solve the left-leg active and passive joint variables given the Cartesian pose ${}^B_P T$, we first equate the given numbers for ${}^B_P T$ with the symbolic form of ${}^B_P T$ as a function of all joint variables:

$$ {}^B_P T_{NUM} = {}^B_P T(\theta_1, \theta_2, \theta_3, L_3, \phi_{2,} \phi_3) \tag{3} $$

The right-hand-side of (3) is the symbolic forward kinematic expressions for the left *SPU* serial chain. Following Craig's (1989) procedure for forming these functions from the DH parameters of Table I will yield ${}^0_8 T$ only; therefore, we need the following equation:

$$ {}^B_P T = {}^B_0 T \, {}^0_8 T \, {}^8_P T \tag{4} $$

where, from Fig. 5:

$$ {}^B_0 T = \begin{bmatrix} 1 & 0 & 0 & 0 \\ 0 & 1 & 0 & -L_1 \\ 0 & 0 & 1 & 0 \\ 0 & 0 & 0 & 1 \end{bmatrix} \qquad {}^8_P T = \begin{bmatrix} 0 & -1 & 0 & -L_5 \\ 1 & 0 & 0 & 0 \\ 0 & 0 & 1 & 0 \\ 0 & 0 & 0 & 1 \end{bmatrix} $$

Equation (4) brings fixed parameters L_1 and L_5 into the process. Since there are six unknowns, the Newton-Raphson method requires six functions for solution. These functions are coupled and non-linear (transcendental); three come from the translational part of (4), and three from the rotational part. Since there are three independent translational terms, we use all three. We define for convenience:

$$ \begin{Bmatrix} X_1 \\ Y_1 \\ Z_1 \end{Bmatrix} = {}^B P_P(\theta_1, \theta_2, \theta_3, L_3, \phi_{2,} \phi_3) \tag{5} $$

These symbolic formulas are in turn equated to known numbers $\{x \quad y \quad z\}^T$ in (4). From the rotation matrix equation part of (4), there are nine possible equations, only three of which are independent due to the orthonormal constraints. We choose the (1,2), (2,2), and (3,3) rotation terms. This yields the following six functions to solve, written so as to equal zero:

$$ \begin{aligned} F_1 &: X_1 - x = 0 \\ F_2 &: Y_1 - y = 0 \\ F_3 &: Z_1 - z = 0 \\ F_4 &: r_{12}^{(1)} + s\alpha c\gamma - c\alpha s\beta s\gamma = 0 \\ F_5 &: r_{22}^{(1)} - c\alpha c\gamma - s\alpha s\beta s\gamma = 0 \\ F_6 &: r_{33}^{(1)} - c\beta c\gamma = 0 \end{aligned} \tag{6} $$

The terms $\{X_1 \quad Y_1 \quad Z_1\}^T$ and $r_{ij}^{(1)}$ are complicated symbolic functions of the unknowns $\Theta = \{\theta_1 \quad \theta_2 \quad \theta_3 \quad L_3 \quad \phi_2 \quad \phi_3\}^T$; we use a computer symbolic manipulation program to assist in their derivations. The $r_{ij}^{(1)}$ terms come from the appropriate elements of the symbolic expressions for ${}^B_P R(\Theta)$. The Cartesian variables (known numbers in the inverse pose problem) all appear explicitly in (6). The translational subscript 1 and rotational superscript (1) indicate left *SPU* leg in Eq. (6). The Newton-Raphson iterative method for solving (6) for the unknowns is summarized now.

Starting from an initial guess for the solution, Θ_0, the Newton-Raphson process for step *k*+1 is summarized below:

- Solve $J_{NR} \delta\Theta_k = -F(\Theta_k)$ for $\delta\Theta_k : \delta\Theta_k = -J_{NR}^{-1} F(\Theta_k)$
- Then $\Theta_{k+1} = \Theta_k + \delta\Theta_k$
- Iterate until $\|\delta\Theta_k\| < \varepsilon$

where $F(\Theta) = \{F_i(\Theta)\}, i = 1,2,\cdots,6$ is given in (6) and ε is a user-defined tolerance (ε can be different for translational and rotational terms), and the Newton-Raphson Jacobian matrix is:

$$ J_{NR} = \left[\frac{\partial F_i}{\partial \Theta_j} \right] \tag{7} $$

Due to the specific *SPU* leg kinematics, this six-by-six Jacobian matrix has zero elements in the (3,1), (6,1), (4,4), (5,4), (6,4), and (6,6) terms. Actually, Gaussian elimination is more robust and efficient than using the matrix inverse above.

In this manner, the inverse pose kinematics problem for the left *SPU* portion of SPAM is solved. The right-leg portion is solved following this, independently in exactly the same manner, using the above-mentioned variable substitutions, symbolic terms $\{X_2 \quad Y_2 \quad Z_2\}^T$ and $r_{ij}^{(2)}$, and unknowns $\Theta = \{\theta_4 \quad \theta_5 \quad \theta_6 \quad L_4 \quad \phi_5 \quad \phi_6\}^T$. We also need to reverse the directions of L_1 and L_5 (see Fig. 4) in the previous transformations:

$$ {}^{B}_{0}T = \begin{bmatrix} 1 & 0 & 0 & 0 \\ 0 & 1 & 0 & L_1 \\ 0 & 0 & 1 & 0 \\ 0 & 0 & 0 & 1 \end{bmatrix} \qquad {}^{8}_{P}T = \begin{bmatrix} 0 & -1 & 0 & L_5 \\ 1 & 0 & 0 & 0 \\ 0 & 0 & 1 & 0 \\ 0 & 0 & 0 & 1 \end{bmatrix} $$

We define for the right leg coupled nonlinear functions F_7 through F_{12} exactly as in (6), but using the index 2 indicating right leg. After the Newton-Raphson method converges for the left leg, we solve the right leg in the same manner, with the differences noted. For real-time control, we are interested only in $\{\theta_1 \quad \theta_2 \quad \theta_3 \quad \theta_4 \quad \theta_5 \quad \theta_6\}^T$, three from the left leg solution and three from the right.

Considering the SPAM complexity we believe Newton-Raphson iteration is the logical choice for solution. However, this method requires a good initial guess for each leg, and results in only one solution. For the Gough/Stewart Platform, there is only one inverse pose solution; for the SPAM there are multiple inverse pose solutions. In practice, these limitations will not be severe since a very good initial guess is available from the previous control cycle and we only want one solution for control of the platform.

This concludes the numerical solution for SPAM inverse pose kinematics, accomplished independently for each *SPU* leg. The next subsection presents the SPAM forward pose kinematics solution.

3.2 Forward Pose Kinematics

The SPAM forward pose kinematics problem is stated: Given the Omni-Wrist actuator joint variables $\{\theta_1 \quad \theta_2 \quad \theta_3 \quad \theta_4 \quad \theta_5 \quad \theta_6\}^T$, calculate the associated Cartesian platform pose $\{x, y, z, \alpha, \beta, \gamma\}$ (or, equivalently, ${}^{B}_{P}T$ as in (2)). The left- and right-leg passive joint variables $\{L_3, \phi_2, \phi_3\}$ and $\{L_4, \phi_5, \phi_6\}$ are again unknowns.

This forward pose problem cannot be solved by considering the left and right *SPU* serial chain legs separately. The problem is coupled because both *SPU* serial chain legs share the same Cartesian unknowns. Standard serial robot kinematics techniques cannot be used in the SPAM forward pose solution since the intermediate passive joint variables are unknown. We will solve this problem in one step via Newton-Raphson iteration.

Since there are twelve unknowns, the Newton-Raphson method requires twelve functions for solution. These functions are the same functions as those developed for inverse pose kinematics in the previous subsection: coupled nonlinear functions F_1 through F_6 for the left *SPU* leg from (6) and similar coupled nonlinear functions F_7 through F_{12} for the right *SPU* leg. The major difference is that now actuator joint variables $\{\theta_1 \quad \theta_2 \quad \theta_3 \quad \theta_4 \quad \theta_5 \quad \theta_6\}^T$ are known, and $\{x, y, z, L_3, \phi_2, \phi_3, \alpha, \beta, \gamma, L_4, \phi_5, \phi_6\}^T$ is now the unknown vector.

The Newton-Raphson method follows the one outlined in the previous subsection for inverse pose kinematics, but now there is a single stage of iterations for twelve transcendental equations coupled in twelve unknowns. A good initial guess for the twelve unknowns is still required. The twelve-by-twelve Newton-Raphson Jacobian matrix is not very difficult to form. Fully 94 of these 144 terms are zero, and six more are negative one (partial derivatives of functions 1,2,3 and 7,8,9 with respect to *x*, *y*, *z*). The partial derivatives of functions 4,5,6 with respect to α,β,γ are the same as those for functions 10,11,12. The remaining terms (partial derivatives of functions 1 through 6 with respect to passive variables $\{L_3, \phi_2, \phi_3\}$ and partial derivatives of functions 7 through 12 with respect to passive variables $\{L_4, \phi_5, \phi_6\}$) were already derived for use in inverse pose kinematics.

Again, the Newton-Raphson approach to solving forward pose kinematics suffers from the need of a good initial guess, and only one of the multiple solutions is found. However, in practice these do not present problems since we know the value of all variables at the previous control cycle.

4. EXAMPLES

This section presents a snapshot example, followed by trajectory examples to demonstrate results from the inverse and forward pose kinematics solutions presented in Section 3.

4.1 A Nominal Configuration

A good nominal configuration for this platform manipulator is a pose like that shown in Fig. 4: the platform is level, {*P*} is translated relative to {*B*} only in the vertical Z direction, and the orientations of {*P*} and {*B*} are aligned (see also Fig. 5). The SPAM design parameters are: L_1 = 0.5334, offset L_2 = 0.0413, and L_5 = 0.3556 (*m*). Choosing a nominal Omni-Wrist angle of $\theta_2 = -10^\circ$ (the wrist doubles this through gear coupling to the upper gimbal shown in Fig. 5, so that the passive length L_3 is aligned -20° from the vertical), the active joint parameters, Cartesian pose, and passive joint variables, respectively, for this configuration are calculated from simple geometry and trigonometry to be:

$$ \begin{aligned} \{\theta_1 \quad \theta_2 \quad \theta_3 \quad \theta_4 \quad \theta_5 \quad \theta_6\} &= \{0 \quad -10 \quad 0 \quad 0 \quad 10 \quad 0\} \\ \{x \quad y \quad z \quad \alpha \quad \beta \quad \gamma\} &= \{0 \quad 0 \quad 0.509 \quad 0 \quad 0 \quad 0\} \\ \{L_3 \quad \phi_2 \quad \phi_3 \quad L_4 \quad \phi_5 \quad \phi_6\} &= \{0.499 \quad 20 \quad 0 \quad 0.499 \quad -20 \quad 0\} \end{aligned} \tag{8} $$

Length units are *m* and angular units are *deg*. We discovered that when the orientations of {*P*} and {*B*} are aligned, the Newton-Raphson procedure experienced great difficulty in finding inverse or forward pose solutions. Perhaps in this case multiple solutions branch together, or a singularity exists. This will require future work to clear up. For now, we simply define a new nominal pose close to the above, but not subject to the same difficulties. This case serves as a snapshot example for both inverse and forward pose kinematics. It was found using a combination of serial forward kinematics for the left leg only, and the numerical parallel inverse kinematics as presented in Section 3. The numerical parallel forward kinematics checked this solution:

$$ \begin{aligned} \{\theta_1 \quad \theta_2 \quad \theta_3 \quad \theta_4 \quad \theta_5 \quad \theta_6\} &= \{1, -10, 1, -7.59, 9.92, 0.99\} \\ \{x \quad y \quad z \quad \alpha \quad \beta \quad \gamma\} &= \{0045, .0005, .5104, 1.65, 1.96, 0.02\} \\ \{L_3 \quad \phi_2 \quad \phi_3 \quad L_4 \quad \phi_5 \quad \phi_6\} &= \{0.50, 20, 1, 0.4999, -20.1, 8.89\} \end{aligned} \tag{9} $$

This second nominal configuration is shown in Fig. 6.

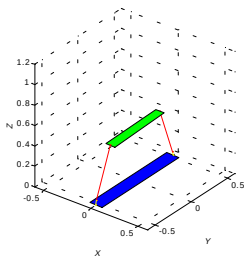

Figure 6. Nominal SPAM Configuration for Examples

4.2 Trajectories with Inverse and Forward Pose Solutions

Starting from the second nominal pose given above, we now present examples for inverse and forward pose solutions that follow simple trajectories, solving the problem at each simulated time step. To demonstrate the *inverse pose solutions*, we start at the Cartesian pose from the middle line of (9). We use the excellent initial guesses (the known solution for all θ_i, plus the known passive variables) for the first time step. For ensuing time steps, the newly found solution is used as the next initial guess. At each step, we add $\{0.005,0.005,0.005,0,0,0.5^\circ\}$ to the specified Cartesian pose. That is, we are translating by 5 *mm* in all *X,Y,Z* axes, and rotating $\gamma = 0.5^\circ$ about the *X* axis at each of ten simulated time steps (starting at zero). The inverse pose solution will be calculated at each control step; since a typical control rate is 100 *Hz*, 5 *mm* is a very large step. Thus, this simulation is more challenging to our algorithm than reality. Figures 7a and 7b present the left and right actuator inverse pose solution results, respectively, for this trajectory example. In Fig. 7a, θ_1 is solid, θ_2 dashed, and θ_3 dotted; in Fig. 7b, θ_4 is solid, θ_5 dashed, and θ_6 dotted.

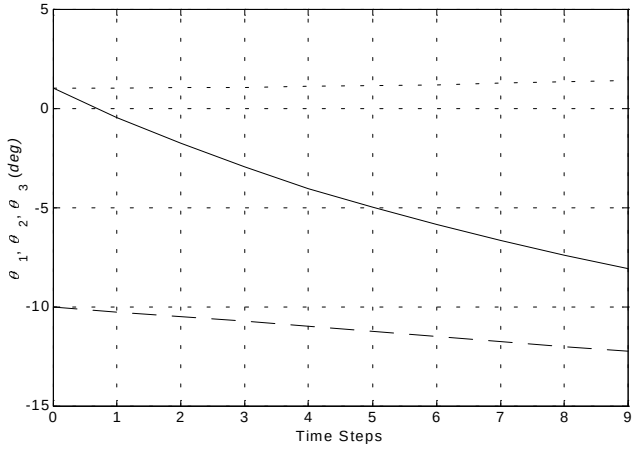

Figure 7a. Inverse Pose Trajectory Results, Left Actuator

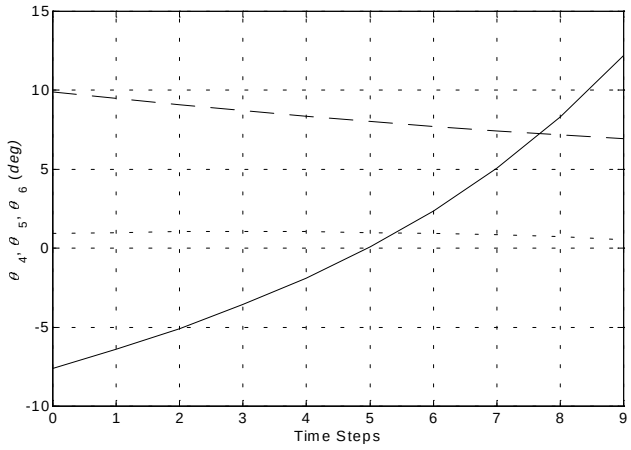

Figure 7b. Inverse Pose Trajectory Results, Right Actuator

The Newton-Raphson tolerances used are ε_T = 0.0001 *m* and ε_R = 0.000001 *rad* for the translational and rotational terms, respectively. Since the example trajectory starts near the (unstable) nominal configuration, the right *SPU* leg requires initially 62 iterations to converge! It then settles on less than 20 iterations for the later time steps. The left *SPU* leg requires around 15 iterations for convergence, despite the excellent initial guesses available. For other examples (not shown) starting further away from this problem configuration, the number of iterations is much lower for convergence (2-5 typically).

To demonstrate the *forward pose solutions*, we again start at the nominal pose of (9). The first active joint input is line 1 of (9), rounded to the nearest whole number (*deg*): $\{1,-10,1,-8,10,1\}$. Line 2 of (9) is an excellent initial guess (along with the known passive variables from (9)) for the forward pose solution in the first time step. For ensuing time steps, the newly found Cartesian pose solution is used as the next initial guess. At each step, we add 0.2° to each of the six active joint angle inputs. Again, this is a large step assuming a typical control rate of 100 *Hz*, and is thus challenging to our algorithm. Figures 8a and 8b present the Cartesian translations and Euler angle results, respectively, for this forward pose trajectory example. In Fig. 8a, *x* is solid, *y* dashed, and *z* dotted (starting from *z* = 0.509 *m*, changing little); in Fig. 8b, α is solid, β dashed, and γ dotted (near zero).

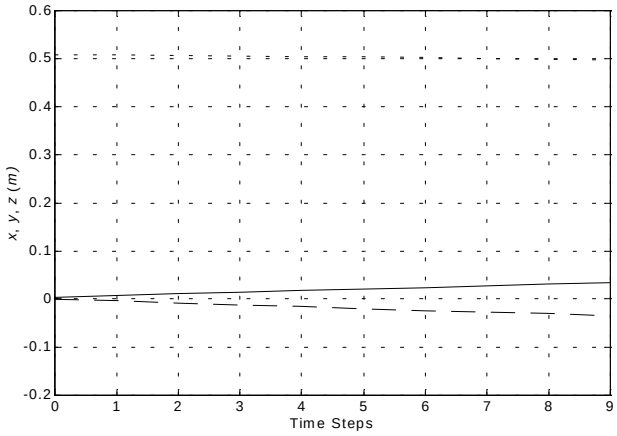

Figure 8a. Forward Pose Trajectory Results, Translations

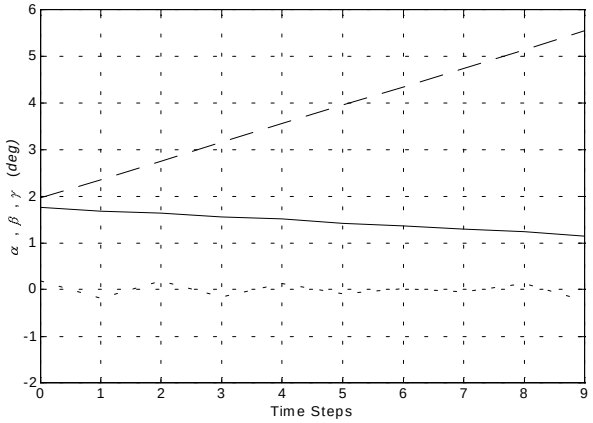

Figure 8b. Forward Pose Trajectory Results, Rotations

The same Newton-Raphson tolerances from the inverse pose solution also used for the forward pose solution. The number of iterations required for convergence is always under 12.

5. CONCLUSION

This paper presents the inverse and forward pose kinematics of a novel platform manipulator, the SPherically-Actuated platform Manipulator, or SPAM. Like the infamous potted meat substitute product, this manipulator may be of lower quality compared with prismatically-actuated platforms, primarily due to moment loading at the actuators. However, there has been significant interest in development of spherical actuators recently, and we wanted to put two Omni-Wrists on loan from NASA to novel use.

SPAM consists of two serial chain legs connecting the moving platform to the fixed base. Two similar versions of SPAM are proposed, one version with *SPU* joints (*S* active, *P-U* passive) and the other version with *SRU* joints (*S* active, *R-U* passive). The inverse and forward pose problems are solved for the *SPU* version in this paper, using numerical Newton-Raphson iteration to solve the coupled transcendental governing equations. The solutions for the *SRU* version are very similar. The inverse pose kinematics, not as straight-forward as the Gough/Stewart platform inverse kinematics, may be solved in two independent steps, one for each serial chain, where the Jacobian matrices order are both six-by-six. The forward pose solutions involve one coupled twelve-by-twelve system. The Newton-Raphson method is limiting since a good initial guess is required and only one of the multiple solutions (both inverse and forward problems have multiple solutions!) is determined. However, as our focus is real-time control of SPAM, this will not present a problem since the previous solution is a good initial guess and only the current solution branch is required.

Examples were presented to demonstrate results from the pose kinematics solution algorithms. It was discovered that at nominal platform orientations where the platform and base orientations align, the pose solution methods experienced great difficulty in converging. This problem must be overcome either by design or alternate solution techniques before SPAM will be a quality platform manipulator. Additional future work plans are in two thrusts. On the theoretical side, the kinematic expressions will be much simplified if true spherical actuators are used, i.e. without the offset present in the Omni-Wrist. It is possible that analytical solutions exist for this simplified case. We are also working on a reduced-order approximate solution by ignoring some of the passive variables to reduce computation. Inverse and forward rate kinematics is also under way. On the practical side, the *SRU* SPAM has been built and we plan to control this hardware in real-time using the inverse pose and resolved-rate (inverse velocity) techniques.

REFERENCES

J.J. Craig, 1989, **Introduction to Robotics: Mechanics and Control**, Addison Wesley Publishing Co., Reading, MA.

K.H. Hunt, 1983, "Structural Kinematics of In-Parallel-Actuated Robot Arms", *Journal of Mechanisms, Transmissions, and Automation in Design*, Vol. 105, No. 4.

K.M. Lee, R.B. Roth, and Z. Zhou, 1996, "Dynamic Modeling and Control of a Ball-joint-Like Variable Reluctance Spherical Motor", *Jnl of Dynamic Systems, Measurement, and Control*, 118(1): 29-40.

M.D. Rhodes and M.M. Mikulas, 1985, "Deployable Controllable Geometry Truss Beam", *NASA Technical Memorandum 86366*.

M.E. Rosheim, 1987, "Singularity-Free Hollow Spray Painting Wrists", *Robots 11 Conference Proceedings RI/SME*, Chicago, IL, 13.7-13.28.

R.B. Roth and K.-M. Lee, 1995, "Design Optimization of a Three Degrees-of-Freedom Variable-Reluctance Spherical Wrist Motor", *Journal of Engineering for Industry*, 117(3): 378-388.

M.M. Stanisic and O. Duta, 1990, "Symmetrically Actuated Double Pointing Systems: The Basis of Singularity-Free Robot Wrists", *IEEE Transactions on Robotics and Automation*, 6(5).

D. Stewart, 1966, *"A Platform with Six Degrees of Freedom"*, Proceedings of the Institute of Mechanical Engineers (London), 180(15): 371-386.

L.-W. Tsai, 1999, **Robot Analysis: The Mechanics of Serial and Parallel Manipulators**, John Wiley & Sons, Inc., New York.

J. Wang, W. Wang, G.W. Jewell, D. Howe, 1998, "Novel Spherical Permanent Magnet Actuator with Three Degrees-of-Freedom", *IEEE Transactions on Magnetics*, 34(4): 2078-2080.

R.L. Williams II, 1999, "Inverse Kinematics and Singularities of Manipulators with Offset Wrist", *IASTED International Journal of Robotics and Automation*, 14(1): 1-8.

R.L. Williams II, 1990, "Forward and Inverse Kinematics of Double Universal Joint Robot Wrists", *Proceedings of the 1990 Space Operations, Applications, and Research (SOAR) Symposium*, Albuquerque, NM.

APPENDIX. *SRU* KINEMATICS PARAMETERS

The body of this paper focused on the SPAM platform manipulator with two *SPU* serial chain legs. The inverse and forward pose kinematics solutions presented may be readily adapted for the SPAM with two *SRU* legs (modeled in Fig. 2). This Appendix briefly presents the model and terms for the *SRU* version. The SPAM kinematic diagram, *SRU* version, is given in Fig. A.1.

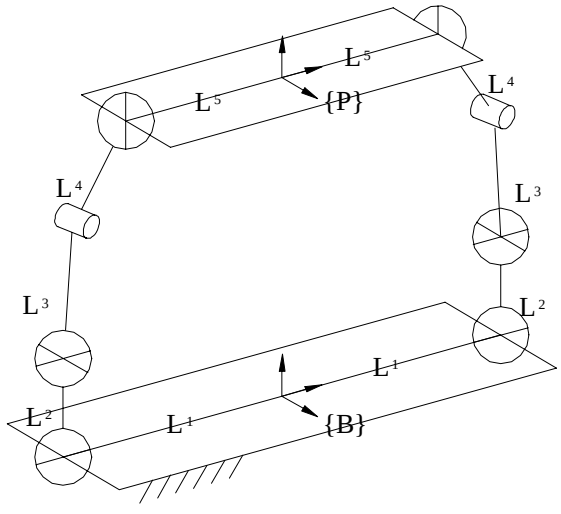

Figure A.1. SPAM Kinematic Diagram, SRU *Version*

Again symmetry is used in design. In Fig. A.1 all lengths $L_i, i = 1,2,\cdots,5$ are rigid. The passive *P*-joints of Fig. 4 are replaced by the passive *R*-joints. The detailed kinematic diagram for the left *SRU* serial chain leg is shown in Fig. A.2. The passive *P*-joint variable L_3 from the *SPU* version is replaced by passive *R*-joint variable ϕ_1. The Denavit-Hartenberg (DH) parameters (Craig, 1989) for the left *SPU* serial chain leg are given in Table A.I (angle units are *deg*). These are identical to the left *SPU* DH parameters given in Table I, with the exception of rows i = 6,7.

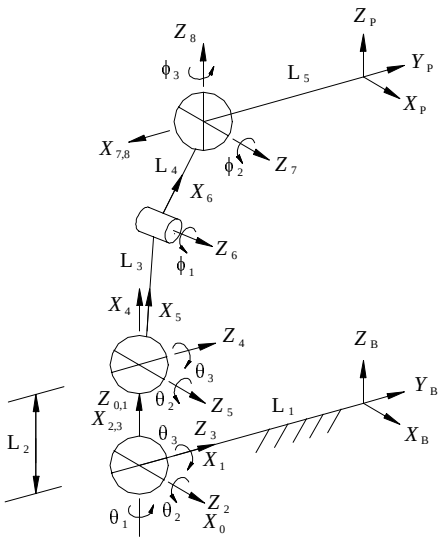

Figure A.2. Left SRU *Leg Kinematic Diagram*

Table A.I. Left *SRU* Leg DH Parameters

i	α_{i-1}	a_{i-1}	d_i	θ_i
1	0	0	0	$\theta_1 + 90$
2	90	0	0	$\theta_2 + 90$
3	90	0	0	θ_3
4	0	L_2	0	θ_3
5	-90	0	0	θ_2
6	0	L_3	0	ϕ_1
7	0	L_4	0	$\phi_2 + 90$
8	90	0	0	ϕ_3

In our design the right *SRU* leg is identical to the left, using the following variable substitutions:

$$\theta_4 \to \theta_1 \qquad \phi_4 \to \phi_1$$
$$\theta_5 \to \theta_2 \qquad \phi_5 \to \phi_2$$
$$\theta_6 \to \theta_3 \qquad \phi_6 \to \phi_3$$

Using the differences noted in this Appendix, the methods of Section 3 may be directly applied to solve the inverse and forward pose kinematics of the SPAM, *SRU* version.